Long-ranged correlations in sheared fluids

James F. Lutsko
Center for Nonlinear Phenomena and Complex Systems, Université Libre de Bruxelles, Campus Plaine, CP 231, 1050 Bruxelles, Belgium

James W. Dufty
Department of Physics, University of Florida, Gainesville, Florida 32611

(Received 17 May 2002; published 14 October 2002)

The presence of long-ranged correlations in a fluid undergoing uniform shear flow is investigated. An exact relation between the density autocorrelation function and the density-mometum correlation function implies that the former must decay more rapidly than $1/r$, in contrast to predictions of simple mode-coupling theory. Analytic and numerical evaluation of a nonperturbative mode-coupling model confirms a crossover from $1/r$ behavior at ''small'' r to a stronger asymptotic power-law decay. The characteristic length scale is $\ell \approx \sqrt{\lambda_0/a}$, where λ_0 is the sound damping constant and a is the shear rate.

DOI: 10.1103/PhysRevE.66.041206 PACS number(s): 05.20.Jj, 05.65.+b, 82.70.Dd

I. INTRODUCTION

Long-range spatial correlations (algebraic decay) in simple classical fluids *at equilibrium* occur only near a thermodynamic critical point, i.e., for finely tuned values of the thermodynamic parameters. On the other hand, such long-range correlations appear generically for a wide class of *nonequilibrium* states [1]. The predictions of this phenomenon have been made in a number of contexts, including self-organized criticality [2], linear response [3], kinetic theory [4], and stochastic hydrodynamics [5]. The simplest and most direct approach is that of linear response where the nonequilibrium correlation functions are expanded about the equilibrium state to first order in a nonequilibrium control parameter (typically a spatial gradient). The algebraic decay is then seen to result from spontaneous excitations of hydrodynamic modes induced by the coupling of the control parameter to an associated flux. A more intuitive analysis of this effect follows from an extension of fluctuating hydrodynamics to nonequilibrium states. To linear order in the control parameter the same algebraic decay is found, as expected. Such theoretical studies for the density autocorrelation function in a fluid subject to a temperature gradient have received detailed experimental confirmation in recent years [6]. The shortest length scale is set by the intermolecular force range, while the experimental verification is on macroscopic system size scales. Since the decay is algebraic there would appear to be no other length scale involved. However, we argue here that there is an additional macroscopic scale set by the parameters of the nonequilibrium state such that the true asymptotic decay is faster than that predicted by simple perturbative studies near equilibrium. The analysis here is limited to a single nonequilibrium state, that of uniform shear flow, but the qualitative features are expected to extend to other nonequilibrium states as well.

Uniform shear flow (USF) is characterized by a constant average density and temperature, and an average velocity flow field given by $\vec{v}(\vec{r}) = \vec{\vec{a}} \cdot \vec{r}$, where the shear rate tensor is traceless ($\vec{\vec{a}} = a y \hat{x}$ in a Cartesian frame of reference). This nonequilibrium state has a single scalar control parameter a and has been the subject of numerous theoretical investigations aimed at understanding transport and fluctuations in a model nonequilibrium state [7–11]. All of these share in common the assumption that at large length and time scales, the dynamics of fluctuations in a simple fluid are dominated by the contribution of the hydrodynamic modes that decay much more slowly than do the neglected kinetic modes. The result is that the decay of thermal fluctuations in the hydrodynamic fields, i.e., the density, momentum, and energy fields, is governed at large length and time scales by equations formally identical to the phenomenological Navier-Stokes equations. Here, ''large length and time scales'' means scales large compared to the mean free path and mean free time, which is the usual domain of validity of hydrodynamics. Correlations between the values of thermally generated fluctuations in the fields at two different space-time points can be modeled by supplementing these equations with random forces, which represent the interaction of this restricted set of variables with the neglected degrees of freedom to give a Langevin model. In equilibrium, the result of the Navier-Stokes-Langevin model is that the equal-time correlation functions for two hydrodynamic fields $x(\vec{r},t)$ and $y(\vec{r},t)$ are simply proportional to the δ-functions in the spatial arguments

$$C_{xy}(\vec{r},\vec{r}') \equiv \langle \delta x(\vec{r},t)\, \delta y(\vec{r}',t) \rangle \to A\, \delta(\vec{r}-\vec{r}'), \qquad (1)$$

where $\delta x = x - \langle x \rangle$, and the amplitude A is a corresponding thermodynamic response function. This result simply confirms that fluctuations at different points in space are uncorrelated when speaking of hydrodynamic length scales (i.e., neglecting correlations on the scale of the force range). In contrast, these correlation functions for the nonequilibrium state have a new long-range component, which to first order in the shear rate is of the form

$$C_{xy}(\vec{r},\vec{r}') \to A\, \delta(\vec{r}-\vec{r}') + aB \frac{1}{|\vec{r}-\vec{r}'|}. \qquad (2)$$

The amplitude B is again a thermodynamic response function. The physical difference between equilibrium and nonequilibrium is due to the way in which small hydrodynamic fluctuations decay. At equilibrium a fluctuation decays locally due to viscous and thermal damping, whereas in shear flow it is convected as well and spreads out over a length scale that varies as the speed of convection times the time scale for viscous and thermal damping [7,8].

With the exception of Ref. [10], the form (2) was generally obtained using a perturbative treatment in Fourier representation assuming that the shear rate a (with dimensions of frequency) is smaller than all other hydrodynamic frequencies ck and $\lambda_0 k^2$, where c is a propagation velocity, λ_0 is a transport coefficient, and k is the wave vector. For fixed shear rate, this therefore sets an upper bound on the range of separations in real space for which the results apply. In this context, the true asymptotic behavior of the correlation functions remains unclear. The analysis of Ref. [10] has the potential to resolve this question since it is nonperturbative and retains the two dominant effects of large shear rate: secular effects $\approx at$ associated with convection, and shear rates comparable to the hydrodynamic damping $a \approx \lambda_0 k^2$. The resulting correlation functions are found to have the form

$$C_{xy}(\vec{r},\vec{r}') \to A\,\delta(\vec{r}-\vec{r}') + aB\frac{1}{|\vec{r}-\vec{r}'|}F((\vec{r}-\vec{r}')/l). \quad (3)$$

The function $F(\vec{r}/l)$ depends on a new nonequilibrium correlation length $l=\sqrt{\lambda_0/a}$. For $r \ll l$ the result (2) is recovered. However, the asymptotic form for $r \gg l$ was not explored in any detail in Ref. [10].

Here, we attempt to clarify the asymptotic behavior of the static correlation functions in a sheared fluid in two ways. First, it is shown that the continuity equation and stationarity place exact constraints on the decay of the density autocorrelation function such that it must be faster than r^{-1} for large r. This result is independent of any model for evaluating the correlation function. Next, we reconsider $F(\vec{r}/l)$ in Eq. (3) from the results of Ref. [10] and show that the actual asymptotic behavior is $r^{-11/3}$. The crossover between the r^{-1} behavior at short length scales and the stronger $r^{-11/3}$ decay at large separations is illustrated by numerical evaluation of the general result.

II. EXACT BOUNDS ON THE RATE OF DECAY

Consider N atoms with positions and momenta denoted by $\vec{q}_i$ and $\vec{p}_i$, respectively, and denoted collectively as $\Gamma = \{\vec{q}_i, \vec{p}_i\}_{i=1}^N$. The atoms interact via a central two-body potential $\phi(r)$ and are confined to a volume V such that the average density is n. The potential is assumed to be repulsive at short distances and to diverge as $r \to 0$ and to have a finite force range. Uniform shear flow results from the application of Lees-Edwards boundary conditions [12] consisting of periodic boundaries in all directions except that of the gradient (here, the y direction). If a particle exits the volume in the positive y direction (say, at $y=L/2$) at time t, it is reentered at the opposite side of the volume ($y=-L/2$) with its velocity in the direction of flow shifted as $v_x \to v_x - aL$ and position shifted as $x \to x - aLt$. Taken together, these constitute periodic boundaries in the local rest frame. The temperature will generally increase due to viscous heating, but we will follow standard practice and assume the presence of a thermostat that counteracts the viscous heating so that the temperature is also constant in time leading to a steady state [13]. The dynamics thus described possess several important symmetries that will be used below. First, they are invariant with respect to parity of the positions and momenta so that the equations of motion and boundary conditions are the same if written in terms of the variables $\tilde{\vec{q}}_i = -\vec{q}_i$ and $\tilde{\vec{p}}_i = -\vec{p}_i$. Second, they are invariant under mirror reflection about the z axis (but not the x or y axes since the boundary condition couples the x velocity and the y coordinate). Third, since USF is a steady state, statistical properties are invariant with respect to a change in the origin from which time is measured (time translational invariance). Fourth, USF is translationally invariant in the local rest frame as well as in a mixed frame consisting of the laboratory positions and the velocities measured relative to the flow [10].

The microscopic local density and momentum fields are defined, respectively, as

$$\psi_n(\vec{r};\Gamma(t;\Gamma_0)) = \sum_{i=1}^N \delta(\vec{r}-\vec{q}_i(t)),$$

$$\vec{\psi}_p(\vec{r};\Gamma(t;\Gamma_0)) = \sum_{i=1}^N \vec{p}_i'(t)\,\delta(\vec{r}-\vec{q}_i(t)), \quad (4)$$

where $\vec{p}_i' = \vec{p}_i - m_i \vec{a}\cdot\vec{q}_i$ is the momentum defined relative to the local flow field and $\Gamma(t;\Gamma_0)$ is the point in phase space, which the system would reach after evolving from the initial point Γ_0 for a time t. Note that these fields are related by the microscopic continuity equation

$$\begin{aligned}\frac{d}{dt}\psi_n(\vec{r};\Gamma(t;\Gamma_0)) &= \sum_{i=1}^N \vec{p}_i(t)\cdot\frac{d}{d\vec{q}(t)}\delta(\vec{r}-\vec{q}_i(t)) \\ &= -\vec{\nabla}\cdot[\vec{\psi}_p(\vec{r};\Gamma(t;\Gamma_0)) \\ &\quad + \vec{a}\cdot\vec{r}\,\psi_n(\vec{r};\Gamma(t;\Gamma_0))]. \quad (5)\end{aligned}$$

The correlations functions are defined as

$$C_{ab}(\vec{r},\vec{r}';t,t') \equiv \int d\Gamma_0 \rho(\Gamma_0)\,\delta\psi_a(\vec{r};\Gamma(t;\Gamma_0))\,\delta\psi_b(\vec{r}';\Gamma(t';\Gamma_0)), \quad (6)$$

where subscripts a and b label the specific field considered, $\rho(\Gamma_0)$ is the distribution of phase variables at initial time $t=0$, and $\delta\psi_a = \psi_a - \langle\psi_a\rangle$. For a steady state the time dependence occurs through $t-t'$ due to time translational invariance. Because of the modified spatial translational invari-

ance, it is also possible to show that the correlation functions depend only on the relative separation. Consequently, the correlation functions can be written as

$$C_{ab}(\vec{r},\vec{r}';t,t') = C_{ab}(\vec{r}-\vec{r}';t-t').$$

Choosing $\vec{r}'=\vec{0}$ and $t'=t$, Eq. (6) gives the relationship

$$\frac{d}{dt}C_{nn}(\vec{r}) = 0 = -\vec{\nabla}\cdot(\vec{C}_{pn}(\vec{r}) - \vec{C}_{np}(\vec{r}) + \vec{a}\cdot\vec{r}C_{nn}(\vec{r})), \quad (7)$$

where for notational simplicity $C_{nn}(\vec{r}) \equiv C_{nn}(\vec{r};0)$. This result has been derived previously in a different context [10]. It simplifies further using the translational, parity, and reflection invariance noted above to give the final form of interest here

$$0 = -\vec{\nabla}\cdot(2\vec{C}_{pn}(\vec{r}) + \vec{a}\cdot\vec{r}C_{nn}(\vec{r})). \quad (8)$$

This is an exact result that follows directly from stationarity and conservation of mass. Integrating (8) over a spherical volume bounded by shells at $r=0^+$ and $r=R$, and making use of Gauss' theorem gives the relationship of $\vec{C}_{pn}(\vec{r})$ to $C_{nn}(\vec{r})$,

$$-2\int \vec{C}_{pn}(R\hat{r})\cdot\hat{r}d\hat{r} = \int \hat{r}\cdot\vec{a}\cdot\vec{r}C_{nn}(R\hat{r})d\hat{r}. \quad (9)$$

The notation $d\hat{r}$ indicates a surface integral over the unit sphere and use has been made of the fact that the correlation functions evaluated at the origin vanish since the potential will not allow atoms to occupy the same spatial position [the singular contribution to $C_{nn} \propto \delta(r)$ is excluded from the integration volume].

Equation (9) is the main result of this section. To put this in context, consider an expansion of $C_{nn}(\vec{r})$ to first order in the shear rate with the form

$$C_{nn}(\vec{r}) \to C_{nn}^{(0)}(r) + \hat{r}\cdot\vec{a}\cdot\hat{r}C_{nn}^{(1)}(r) + o(a^2). \quad (10)$$

Inserting this into Eq. (9) gives

$$-2\int \vec{C}_{pn}(R\hat{r})\cdot\hat{r}d\hat{r} \to a^2\frac{4\pi}{15}RC_{nn}^{(1)}(R) + o(a^3), \quad (11)$$

showing that if the density-momentum correlation function decays for large separations, as it must, then the first-order correction to the density-density correlation function must decay faster than $1/R$. This result is independent of the dimensionality of the system. Furthermore, multiplying Eq. (9) by R^{D-1} and integrating gives, in D dimensions,

$$\int \vec{C}_{pn}(\vec{r})\cdot\hat{r}d^Dr = \int_\Omega \hat{r}\cdot\vec{a}\cdot\hat{r}rC_{nn}(\vec{r})d^Dr = a^2\frac{4\pi}{15}\int_0^\infty r^D C_{nn}^{(1)}(r)dr + o(a^3). \quad (12)$$

The quantity on the left is

$$\int \vec{C}_{pn}(\vec{r})\cdot\hat{r}d^Dr = \left\langle \sum_{i<j} \vec{p}'_{ij}\cdot\hat{q}_{ij} \right\rangle, \quad (13)$$

which vanishes in equilibrium but can be finite for USF due to velocity correlations. This in turn implies that the first-order correction to the shear rate decays faster than $1/r^{D+1}$.

These results can be given a somewhat more general interpretation. Any function of a vector can be expanded in terms of the spherical harmonics in order to separate the dependence of the function on the direction and magnitude of its argument. The density-density correlation function becomes

$$C_{nn}(\vec{r}) = \sum_{L=0}^{\infty}\sum_{M=-L}^{L} C_{nn}^{LM}(r)Y_{LM}(\hat{r}), \quad (14)$$

with

$$C_{nn}^{LM}(r) = \int d\hat{r}Y_{LM}^*(\hat{r})C_{nn}(\vec{r}). \quad (15)$$

Because of the parity symmetry of USF, it is easy to show that only coefficients with even values of L are nonzero, while the inversion symmetry about the z axis implies that only even values of M contribute. Then, noting that

$$\hat{r}_x\hat{r}_y = -i\sqrt{\frac{2\pi}{15}}(Y_{22}(\hat{r}) - Y_{22}^*(\hat{r})), \quad (16)$$

Eq. (9) becomes

$$\int \vec{C}_{pn}(R\hat{r})\cdot\hat{r}d\hat{r} = -2a\sqrt{\frac{2\pi}{15}}R\,\mathrm{Im}C_{nn}^{22}(r). \quad (17)$$

The conclusions drawn about the first-order correction $C_{nn}^{(1)}(r)$ are seen to be exact statements also about $\mathrm{Im}C_{nn}^{22}(r)$, valid to *all* orders in the shear rate: namely, that $\mathrm{Im}C_{nn}^{22}(r)$ must decay faster than $1/r$ in any number of dimensions and faster than $1/r^{D+1}$ in D dimensions if the spatial integral of the radial part of the density-momentum correlation function is finite. This corresponds precisely to the quantity for which the first-order results (2) predicted a $1/r$ decay. Consequently, that result cannot be correct for sufficiently large r.

III. APPROXIMATE EVALUATION OF $C_{nn}(\vec{r})$

The algebraic decays of both static and dynamic correlation functions observed in simple fluids can be derived by means of fluctuating hydrodynamics. In this model, the exact conservation laws for the local density, momentum, and energy density fields, (ρ,$\vec{p}$ and u), respectively,

$$\frac{\partial}{\partial t}\rho + \vec{\nabla}\cdot\vec{p} = 0,$$

$$\frac{\partial}{\partial t}\vec{p} + \vec{\nabla}\cdot\vec{P} = 0,$$

$$\frac{\partial}{\partial t}u+\vec{\nabla}\cdot\vec{q}=0, \tag{18}$$

are approximated by taking the pressure tensor $\overleftrightarrow{P}$ and heat flux vector $\vec{q}$ to be a sum of two terms: the usual Navier-Stokes functionals of the local fields, and a random component that is δ-function correlated in space and time. The amplitudes of these correlations are related to the forms of the deterministic parts of the fluxes [14]. Rewriting these in terms of deviations from the macroscopic state then gives a description of fluctuations about this state. The details for USF have been discussed in detail elsewhere [10] and only the results are quoted for the purposes here. Defining the Fourier transform of the density-density correlation function as

$$\tilde{C}_{nn}(\vec{k})=\int d\vec{r}\,\exp(i\vec{k}\cdot\vec{r})C_{nn}(\vec{r}), \tag{19}$$

the result obtained for it is

$$\tilde{C}_{nn}(\vec{k};a)=k_BT_0\rho_0^2\chi_T(1+\gamma^{-1}\tilde{\Delta}_{nn}(\vec{k}l)), \tag{20}$$

$$\tilde{\Delta}_{nn}(\vec{k})=\int_0^\infty ds\frac{kk_xk_y(-s)}{k^3(-s)}\exp\left(-\int_0^s ds'k^2(-s')\right). \tag{21}$$

Here χ_T is the isothermal compressibility, $\gamma=c_p/c_V$ is the ratio of specific heats at constant pressure and volume, and $\vec{k}(t)=(k_x,k_y-tk_x,k_z)$. The characteristic length scale is $l=\sqrt{\lambda_0/a}$, where λ_0 is the equilibrium sound-damping constant. The first term in Eq. (20) is the equilibrium contribution which, in the small wave vector approximation used here, is a constant. The second term represents the nonequilibrium correction which is derived assuming that the shear rate and rate of dissipation are significantly less than the sound frequency $a,\lambda_0k^2\ll c_0k$, where c_0 is the speed of sound. However, no restriction on the value of a/λ_0k^2 is imposed. The inverse transform of Eq. (20) is the real space result quoted in Eq. (3) above.

In order to evaluate the behavior in real space, it is useful to introduce the expansion of $\tilde{C}_{nn}(\vec{k})$ in spherical harmonics,

$$\tilde{C}_{nn}(\vec{k})=\sum_{L=0}^{\infty}\sum_{M=-L}^{L}\bar{C}_{nn}^{LM}(k)Y_{LM}(\hat{k}), \tag{22}$$

and to recall the relation between the coefficients (15) to those in Eq. (22),

$$C_{nn}^{LM}(r)=\frac{1}{2\pi^2i^L}\int_0^\infty k^2dkj_L(kr)\bar{C}_{nn}^{LM}(k). \tag{23}$$

This gives directly

$$C_{nn}^{LM}(r)=(k_BT_0\rho_0^2\chi_T)\sqrt{4\pi}l^{-3}\delta(\vec{r}/l)\,\delta_{L0}\delta_{M0}+(k_BT_0\rho_0^2\chi_T\gamma^{-1})\frac{1}{2\pi^2i^L}l^{-3}\Delta_{nn}^{LM}(r/l), \tag{24}$$

with

$$\Delta_{nn}^{LM}(\rho=r/l)=\int d\vec{k}j_L(k\rho)Y_{LM}^*(\hat{k})\int_0^\infty ds\frac{kk_xk_y(-s)}{k'^3(-s)}\exp\left(-\int_0^s ds'k^2(-s')\right)=\left(\frac{1}{\rho}\right)\int d\vec{k}j_L(k)Y_{LM}^*(\hat{k})\times\int_0^\infty ds\frac{kk_xk_y(-s\rho^2)}{k^3(-s\rho^2)}\exp\left(-\int_0^s ds'k^2(-s'\rho^2)\right). \tag{25}$$

The small shear rate limit (2) is obtained by noting that l^2 is inversely proportional to the shear rate and expanding to leading order in a,

$$l^{-3}\Delta_{nn}^{LM}(r/l)\to l^{-3}\left(\frac{l}{r}\right)\left[-\int d\vec{k}j_L(k)Y_{LM}^*(\hat{k})\frac{k_xk_y}{k^4}\right]\to\frac{a}{\lambda_0 r}\left[i\delta_{L2}(\delta_{M2}-\delta_{M-2})\frac{\pi}{4}\sqrt{\frac{2\pi}{15}}\right]. \tag{26}$$

The context here shows that this result applys only in the limit $r/l\to0$, which is to say that, for fixed shear rate, this is a *small r* result and does not represent the true long-range behavior of the correlation function.

The actual asymptotic behavior for large $\rho=r/l$ is obtained in the Appendix where it is found that

$$\Delta_{nn}^{00}(\rho)\to\left(\frac{2}{9}\right)^{2/3}5\pi\Gamma\left(\frac{5}{6}\right)\rho^{-11/3}+O(\rho^{-13/3})\approx6.5\rho^{-11/3}. \tag{27}$$

All other components decay even more rapidly. In particular, the true asymptotic behavior of $\mathrm{Im}\Delta_{nn}^{22}(x)$ is found to be

$$\mathrm{Im}\Delta_{nn}^{22}(\rho)\to\frac{935}{756}6^{1/6}\sqrt{5}\pi\Gamma\left(\frac{5}{6}\right)\rho^{-17/3}+O(\rho^{-19/3})\approx13.2\rho^{-17/3}. \tag{28}$$

This is consistent with the exact result (17) that this component must decay more slowly than r^{-4} in three dimensions.

In order to probe the asymptotic behavior in more detail, we have performed a numerical evaluation of Eq. (25) by means of multidimensional Monte Carlo integration using the VEGAS algorithm [15–17]. Rather than directly evaluating Eq. (25), it was found to be more efficient to separate out the short-ranged $1/r$ behavior by rewriting this as

$$\Delta_{nn}^{LM}(\rho)=-i\delta_{2l}(\delta_{m2}-\delta_{m-2})\sqrt{\frac{2\pi}{15}}\frac{\pi}{4\rho}+\int d\vec{k}j_L(k\rho)Y_{LM}^*(\hat{k})\times\int_0^\infty ds\left(\frac{kk_xk_y(-s)}{k^3(-s)}-\frac{k^2(-s)k_xk_y}{k^4}\right)$$
$$\times\exp\left(-\int_0^s ds'k^2(-s')\right). \tag{29}$$

The number of samples used in performing the integrals was adjusted so that the internal estimate of the error in the evaluations was always less than 5% of the calculated values. For small ρ, the errors were substantially less while the limit was occasionally reached as ρ was increased. Figure 1 shows the spherically averaged value $\Delta_{nn}^{00}(\rho)$ as a function of ρ together with the asymptotic power law of $-11/3$, and the two are seen to be consistent. Figure 2 shows the numerical calculation $\Delta_{nn}^{22}(\rho)$ in comparison with the small- and large-r limits, [Eqs. (26) and (28)], respectively. Again, crossover between the limiting forms is clearly identified.

IV. DISCUSSION

The prediction of $1/r$ decays in the density autocorrelation function in shear flow is in violation of an exact bound coming from elementary considerations of statistical mechanics and the properties of the USF steady state. Detailed analysis of a less restrictive solution of the Navier-Stokes-Langevin model confirms that the $1/r$ behavior is actually valid only for $r<\sqrt{\lambda_0/a}$ and that this crosses over to a stronger power-law decay at large distances. It turns out for this model that the density-energy correlation function as well as energy and longitudinal-velocity autocorrelation functions share the same spatial dependence given by Eq. (26). Therefore the calculations given here apply to them as well. Interestingly, the most long-ranged correlation function, based on calculations analogous to that illustrated in the Appendix, is for one of the transverse-velocity autocorrelations which, in the notation of Ref. [10], has the form

$$C_{44}(\vec{r})=k_BT_0[1+\Delta_{44}(\vec{r}/l')] \tag{30}$$

with $l'=\sqrt{2\nu_0/a}$, where ν_0 is the shear viscosity and

$$\Delta_{44}^{00}(\rho)\to\frac{1}{5}6^{2/3}\pi\Gamma\left(\frac{5}{6}\right)\rho^{-5/3}+O(\rho^{-7/3}). \tag{31}$$

To put these results in perspective, we can calculate the crossover length scale for several relevant systems using the Enskog (hard-sphere) model for the transport coefficients. In this case, for all densities and choices of transport coefficients, one has that $\lambda_0\tau/l_{mfp}^2\sim O(1)$, where l_{mfp} is the mean free path and τ is the mean free time, giving $l\sim l_{mfp}/\sqrt{a\tau}$. For water at standard temperature and pressure, the mean free time is of the order of 10^{-12} s and the mean free path is on the order of 10^{-7} cm so that $l\sim 10^{-1}$ cm$/\sqrt{a}$, where the

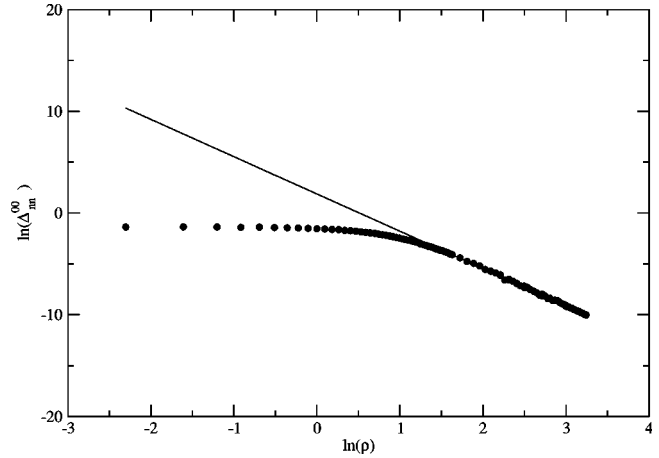

FIG. 1. $\ln(\Delta_{nn}^{00})$ as a function of $\ln(r/l)$ as determined by the numerical calculation (circles) and the asymptotic result given in Eq. (27) (line).

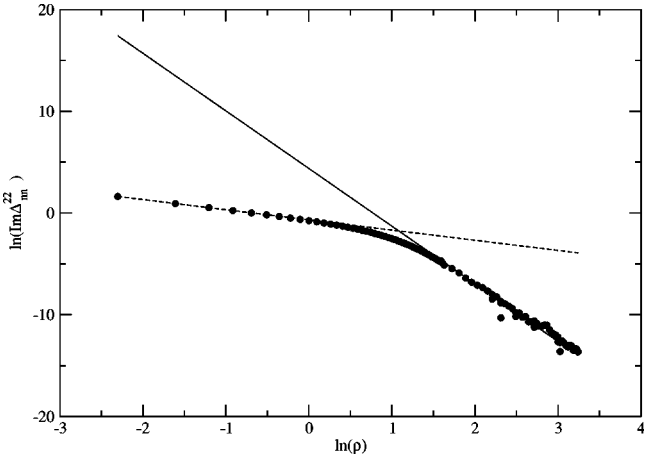

FIG. 2. $\ln(\mathrm{Im}\Delta_{nn}^{22})$ as a function of $\ln(r/l)$ as determined by the numerical calculation (circles) and the asymptotic results given in Eq. (28) (full line) and Eq. (26) (dotted line).

shear rate is expressed in Hz. The crossover length is therefore macroscopic for shear rates that are experimentally feasible (say, shear rates less than 1 KHz). On the other hand, in colloidal suspensions, typical parameters are [18] $\tau \sim 10^{-2} s$ and $l_{mfp} \sim 10^{-5}$ cm giving $l \sim 10^{-4}$ cm$/\sqrt{a}$ or within an order of magitude of the mean free path. In computer simulations, the accessible values of the shear rate typically are in the range $0.01 < a\tau < 10$, so that the relevant length scale is again $0.1 < l/l_{mfp} < 10$. Since the Navier-Stokes model is only valid for spatial scales much larger than the mean free path, this means that the short-ranged $1/r$ behavior would be relevant for water, but only the weaker asymptotic behavior is relevant for the other two systems.

The analysis here has implicitly assumed stability of the USF state. In fact, USF is unstable to sufficiently long wavelength perturbations [11,19]. The critical wavelength for stability scales approximately as v_T/a for small a, where v_T is the thermal velocity. Therefore in order to see the crossover phenomenon discussed here, there must be conditions such that $l \ll v_T/a$. This requires $a\lambda_0/v_T^2 \ll 1$, which can be accomplished by small shear rates and high temperatures. The predicted behavior should be accessible via molecular dynamics simulation for a sufficiently large system.

The qualitative feature of a nonequilibrium length scale should be more general than the special case of USF, and applicable to other nonequilibrium states as well. For example, a steady state with uniform temperature gradient has a characteristic frequency $v_T \nabla \ln T$. Setting this equal to a hydrodynamic damping gives the length scale $l = \sqrt{\lambda_0/(v_T \nabla \ln T)}$. It is expected that the asymptotic decay for $r \gg l$ will be different from that of perturbative mode-coupling theory currently in the literature for reasons similar to those given here for USF.

ACKNOWLEDGMENTS

J. F. Lutsko acknowledges support from the Université Libre de Bruxelles. The research of J. Dufty was supported in part by U. S. Department of Energy Grant No. DE-FG03-98DP00218.

APPENDIX ASYMPTOTIC BEHAVIOR OF THE CORRELATION FUNCTIONS

We begin by writing

$$\tilde{\Delta}_{nn}(\vec{k}) = \int_0^\infty dt \frac{\hat{k}_x\hat{k}_y + t\hat{k}_x^2}{(1+2\hat{k}_x\hat{k}_y t + \hat{k}_x^2 t^2)^{3/2}} \exp[-k^2\beta(t)], \tag{A1}$$

where $\beta(t) = t + \hat{k}_x\hat{k}_y t^2 + \frac{1}{3}\hat{k}_x^2 t^3$ is independent of the magnitude of the wave vector. The coefficients of the expansion in spherical harmonics in real space are then

$$\Delta_{nn}^{LM}(\rho) = \int d\hat{k} Y_{LM}^*(\hat{k}) \int_0^\infty dk k^2 j_L(k\rho) \int_0^\infty dt \frac{\hat{k}_x\hat{k}_y + t\hat{k}_x^2}{(1+2\hat{k}_x\hat{k}_y t + \hat{k}_x^2 t^2)^{3/2}} \exp[-k^2\beta(t)] = \sqrt{\pi} \frac{\Gamma\left(\frac{L+3}{2}\right)}{2^{L+2}\Gamma\left(\frac{2L+3}{2}\right)} \rho^{-3} \int d\hat{k} Y_{LM}^*(\hat{k})$$

$$\times \int_0^\infty dt \frac{\hat{k}_x\hat{k}_y + t\hat{k}_x^2}{(1+2\hat{k}_x\hat{k}_y t + \hat{k}_x^2 t^2)^{3/2}} \left(\frac{\rho^2}{\beta(t)}\right)^{L+3/2} M\left(\frac{L+3}{2}, \frac{2L+3}{2}, -\frac{\rho^2}{4\beta(t)}\right), \tag{A2}$$

where $M(a,b,z)$ is the confluent hypergeometric function. Now, changing variables to $t = \rho^{2/3}(\hat{k}_x^2)^{-1/3} y^{-1}$ gives

$$\Delta_{nn}^{LM}(\rho) = \sqrt{\pi} \frac{\Gamma\left(\frac{L+3}{2}\right)}{2^{L+2}\Gamma\left(\frac{2L+3}{2}\right)} r^{-11/3} \int d\hat{k} Y_{LM}^*(\hat{k}) (\hat{k}_x^2)^{-1/6} \int_0^\infty dy \frac{1 + \hat{k}_x\hat{k}_y (\hat{k}_x^2)^{-2/3} y \rho^{-2/3}}{(1 + 2\hat{k}_x\hat{k}_y (\hat{k}_x^2)^{-2/3} y\rho^{-2/3} + (\hat{k}_x^2)^{-1/3} y^2 \rho^{-4/3})^{3/2}}$$

$$\times \left(\frac{y^3}{\gamma(y)}\right)^{L+3/2} M\left(\frac{L+3}{2}, \frac{2L+3}{2}, -\frac{y^3}{4\gamma(y)}\right), \tag{A3}$$

with

$$\gamma(y) = \frac{1}{3} + \hat{k}_x\hat{k}_y (\hat{k}_x^2)^{-2/3} y\rho^{-2/3} + (\hat{k}_x^2)^{-1/3} y^2 \rho^{-4/3}. \tag{A4}$$

For the 00 component, we use $M(a,a,z) = \exp(z)$ to get

$$\Delta_{ab}^{00}(\rho) = \frac{1}{2^3}\rho^{-11/3} \int d\hat{k} (\hat{k}_x^2)^{-1/6} \int_0^\infty dy (3y^3)^{3/2} \exp\left(-\frac{3y^3}{4}\right) + O(\rho^{-13/3}) = 2^{2/3} 3^{-4/3} 5\pi \Gamma\left(\frac{5}{6}\right) \rho^{-11/3} + O(\rho^{-13/3}). \tag{A5}$$

For the 22 component, it is more convienient to go back to the beginning and to integrate by parts

$$\Delta_{nn}^{LM}(\rho)=\int d\hat{k}Y_{LM}^{*}(\hat{k})\int_0^\infty k^2dkj_L(k\rho)\int_0^\infty dt\left[-\frac{d}{dt}(1+2\hat{k}_x\hat{k}_yt+\hat{k}_x^2t^2)^{-1/2}\right]\exp[-k^2\beta(t)]$$

$$=\rho^{-3}\int d\hat{k}Y_{LM}^{*}(\hat{k})\int_0^\infty k^2dkj_L(k)-\sqrt{\pi}\frac{\Gamma\left(\frac{L+5}{2}\right)}{2^{L+2}\Gamma\left(L+\frac{3}{2}\right)}\rho^{-5}\int d\hat{k}Y_{LM}^{*}(\hat{k})\int_0^\infty dt(1+2\hat{k}_x\hat{k}_yt+\hat{k}_x^2t^2)^{1/2}$$

$$\times\left(\frac{\rho^2}{\beta(t)}\right)^{(1/2)L+(5/2)}M\left(\frac{L+5}{2},\frac{2L+3}{2},-\frac{\rho^2}{4\beta(t)}\right). \tag{A6}$$

The first term vanishes for $L>1$ so

$$\mathrm{Im}\Delta_{nn}^{22}(\rho)=-\sqrt{\pi}\frac{1}{2^4}\rho^{-5}\int d\hat{k}\mathrm{Im}Y_{22}^{*}(\hat{k})\int_0^\infty dt(1+2\hat{k}_x\hat{k}_yt+\hat{k}_x^2t^2)^{1/2}\left(\frac{\rho^2}{\beta(t)}\right)^{7/2}\exp\left(-\frac{\rho^2}{4\beta(t)}\right), \tag{A7}$$

and making the same change of variables as above gives

$$\mathrm{Im}\Delta_{nn}^{22}(\rho)=-\sqrt{\pi}\frac{1}{2^4}\rho^{-11/3}\int d\hat{k}\mathrm{Im}Y_{22}^{*}(\hat{k})(\hat{k}_x^2)^{-1/6}\int_0^\infty y^{-3}dy(1+2\hat{k}_x\hat{k}_y\rho^{-2/3}(\hat{k}_x^2)^{-2/3}y+\rho^{-4/3}(\hat{k}_x^2)^{-1/3}y^2)^{1/2}$$

$$\times\left(\frac{y^3}{\gamma(y)}\right)^{7/2}\exp\left(-\frac{y^3}{4\gamma(y)}\right). \tag{A8}$$

Now, only the odd terms in $\hat{k}_x\hat{k}_y$ give nonvanishing contributions so we expand as

$$(1+2\hat{k}_x\hat{k}_y\rho^{-2/3}(\hat{k}_x^2)^{-2/3}y+\rho^{-4/3}(\hat{k}_x^2)^{-1/3}y^2)^{1/2}\left(\frac{y^3}{\gamma(y)}\right)^{7/2}\exp\left(-\frac{y^3}{4\gamma(y)}\right)$$

$$=\frac{27}{4}\sqrt{3}\hat{k}_x\hat{k}_y(\hat{k}_x^2)^{-2/3}(9y^3-38)y^{23/2}\exp\left(-\frac{3}{4}y^3\right)\rho^{-2/3}+\frac{27}{128}\sqrt{3}y^{27/2}\hat{k}_x\hat{k}_y(\hat{k}_x^2)^{-2}$$

$$\times\exp\left(-\frac{3}{4}y^3\right)\rho^{-2}[8(\hat{k}_x^2)(-918y^3+81y^6+2008)+(\hat{k}_x\hat{k}_y)^2(28\,044y^3-5022y^6+243y^9-40\,088)]+O(r^{-8/3})+\text{even}. \tag{A9}$$

The y integral of the first term vanishes and the next term gives

$$\mathrm{Im}\Delta_{nn}^{22}(\rho)=\frac{935}{729}3^{2/3}\sqrt{\pi}2^{2/3}\Gamma\left(\frac{5}{6}\right)\rho^{-17/3}\int d\hat{k}\mathrm{Im}Y_{lm}^{*}(\hat{k})(\hat{k}_x^2)^{-1/6}\hat{k}_x\hat{k}_y(\hat{k}_x^2)^{-2}(3(\hat{k}_x^2)-2(\hat{k}_x\hat{k}_y)^2)$$

$$=\frac{935}{756}3^{2/3}\sqrt{302}^{2/3}\pi\Gamma\left(\frac{5}{6}\right)\rho^{-17/3}. \tag{A10}$$

[1] J.R. Dorfman, T. Kirkpatrick, and J.V. Sengers, Annu. Rev. Phys. Chem. **45**, 213 (1994); T. Kirkpatrick, D. Belitz, and J. Sengers, e-print cond-mat/0110603.

[2] G. Grinstein, D.-H. Lee, and S. Sachdev, Phys. Rev. Lett. **64**, 1927 (1990).

[3] J. Dufty, in *Spectral Line Shapes*, edited by B. Wende (Gruyter, New York, 1981), p. 1143; Ann. N.Y. Acad. Sci. **848**, 1 (1998).

[4] T.R. Kirkpatrick, E.G.D. Cohen, and J.R. Dorfman, Phys. Rev. A **26**, 972 (1986).

[5] R. Schmitz, Phys. Rep. **171**, 1 (1988).

[6] W.B. Lee, P.N. Segrè, R.W. Gammon, and J.V. Sengers, Physica A **204**, 399 (1994).

[7] J. Machta, I. Oppenheim, and I. Procaccia, Phys. Rev. A **22**, 2809 (1980).

[8] A.-M.S. Tremblay, M. Arai, and E.D. Siggia, Phys. Rev. A **23**, 1451 (1981).

[9] L.S. Garcia-Colin and R.M. Velesco, Phys. Rev. A **26**, 2187

(1982).
[10] J. Lutsko and J.W. Dufty, Phys. Rev. A **32**, 3040 (1985); in *Recent Developments in Nonequilibrium Thermodynamics*, edited by J. Casas-Vazques, Lecture Notes in Physics Vol. 253 (Springer-Verlag, Berlin, 1986).
[11] M. Lee and J.W. Dufty, Phys. Rev. E **56**, 1733 (1997).
[12] A. Lees and S. Edwards, J. Phys. C **5**, 1921 (1972).
[13] W. Hoover, Annu. Rev. Phys. Chem. **34**, 103 (1983); D. Evans and G. Morriss, Comput. Phys. Rep. **1**, 299 (1984).
[14] W. van Saarloos, D. Bedeaux, and P. Mazur, Physica A **110**, 147 (1982); V. Morozov, *ibid.* **126**, 443 (1984).
[15] G.P. Lepage, J. Comput. Phys. **27**, 192 (1978).
[16] W. H. Press, S. A. Teukolsky, W. T. Vetterling, and B. P. Flannery, *Numerical Recipes in C* (Cambridge University Press, Cambridge, 1993).
[17] The Gnu Scientific Library, http://sources. redhat. com/gsl
[18] Noel A. Clark and Bruce J. Ackerson, Phys. Rev. Lett. **44**, 1005 (1980).
[19] M. Lee, J.W. Dufty, J.M. Montanero, A. Santos, and J.F. Lutsko, Phys. Rev. Lett. **76**, 2702 (1996); J.M. Montanero, A. Santos, M. Lee, J.W. Dufty, and J.F. Lutsko, Phys. Rev. E **57**, 546 (1998).